

Numerical Calculation of the Tee Local Resistance Coefficient

Qin Zhang¹, Manlai Zhang¹, Zhihong Zhou¹ and Shizhong Wei^{*2}

¹School of Mechanical Engineering, Yangtze University, Jingzhou, Hubei, 434023, China

²School of Materials Science and Engineering, Henan University of Science and Technology, Luoyang, Henan, 471023, China

Abstract: The local head loss of tee could be calculated with the determination of local resistance coefficient by CFD simulation and test. Based on the mesh-independent feature identified, the flow field inner tee was numerically simulated by the standard k - ε turbulent model and SIMPLEC algorithms, which has revealed the mainstream was obliged to turn to the opposite side of tee junction, and a rise in pressure drop between upstream and downstream was caused as a result. Furthermore, the frictional resistance coefficient was calculated for eliminating the frictional head loss of model, which decreased from 0.0207 to 0.0133 when the inlet velocity increased from 1 m/s to 12 m/s. Additionally, the local resistance coefficients of tee at flow conditions were attained, and the quadratic polynomial between the local resistance coefficient and flux ratio was presented due to the influence of branch on mainstream. Through the test, the simulation result has been compared and the effectiveness of simulation has been verified.

Keywords: CFD, flow field, local resistance coefficient, numerical simulation, tee.

1. INTRODUCTION

As a kind of pipe fittings, tee is widely used in the petrochemical industry. When fluid flow through the tee, the fluid velocity in the tee is redistributed for fluid particles turbulently fluctuate, and local energy loss is caused during energy transfer. Determining the local head loss is the key of hydraulic calculation of pipeline. In general, the local resistance coefficient of the tee is regarded as a constant for convenience, and this will cause larger calculation error because local resistance coefficient changes at different flow patterns for the same tee. To precisely compute the local head loss, the coefficient is needed to be studied. Wu Shengmin *et al.* [1] obtained the local resistance coefficient of DN50 standard tee at different velocity through experiments. Jorgen *et al.* [2] found that the local resistance coefficient was related with the flow pattern and the flux ratio through the test and simulation of tee. Additionally, other previous works [3-5] also drew similar conclusion, and the methods of simulation and experiment were used to study the flow characteristic of Y-type tube [6,7].

In theory, it may connect up to 65000 temperature detection module under each Zigbee gateway of the system, and there is no restriction on amount of Zigbee gateway, and theoretically it may detect several thousand even over ten thousand greenhouse temperature, and the system can not only check current temperature of the greenhouse in real time whenever and wherever, but also give warning in case of too low or high temperature. The reachable distance of Zigbee network may be increased to 3000 m through

increasing transmit power, and it is applicable to agricultural production of temperature greenhouses in large area.

In this paper, the internal flow field of tee is simulated with the Computational Fluid Dynamics method (CFD) to investigate the cause of local head loss for tee, and the pressure drops at different velocities are gotten to calculate the local resistance coefficient for tee.

2. CFD MODEL AND COMPUTATIONAL METHOD

2.1. Fluid Flow Model

To simulate the flow field, the conservation equations for mass and momentum in combination with transport equations for turbulence model are computed.

Assuming that the pipe flow is three-dimensional, incompressible flow, the equation for conservation of mass can be written as

$$\frac{\partial \rho}{\partial t} + \frac{\partial(\rho u_j)}{\partial x_j} = 0 \quad (1)$$

where ρ is the fluid density and u_j is the average velocity component.

Momentum equation is written as

$$\frac{\partial}{\partial t}(\rho p u_i) + \frac{\partial}{\partial x_j}(\rho p u_i u_j) = \rho F_i - \frac{\partial p}{\partial x_i} + \frac{\partial}{\partial x_j}(\mu \frac{\partial u_i}{\partial x_j}) - \frac{\partial}{\partial x_j}(\rho u_i' u_j') \quad (2)$$

where p is the static pressure and the stress tensor is expressed as

$$-\rho u_i' u_j' = \mu_i \left[\left(\frac{\partial u_i}{\partial x_j} + \frac{\partial u_j}{\partial x_i} \right) - \frac{2}{3} \frac{\partial u_j}{\partial x_j} \delta_{ij} \right] \quad (3)$$

where δ_{ij} is the Kronecker delta and the turbulent viscosity, μ_t is eddy diffusivity expressed in the high-Reynolds number form as

$$\mu_t = \rho C_\mu \frac{k^2}{\varepsilon} \tag{4}$$

where k and ε are respectively the kinetic energy and dissipation rate of turbulence, they can be written as

$$k = \frac{\overline{u'_i u'_i}}{2} \tag{5}$$

$$\varepsilon = \frac{\mu}{\rho} \overline{\left(\frac{\partial u'_i}{\partial x_j} \right) \cdot \left(\frac{\partial u'_i}{\partial x_j} \right)} \tag{6}$$

As above equations are not closed, standard $k - \varepsilon$ turbulent model [8] is applied for turbulence modeling. The k and ε are obtained from the following transport equations

$$\frac{\partial(\rho k)}{\partial t} + \frac{\partial(\rho k u_j)}{\partial x_j} = \frac{\partial}{\partial x_j} \left[\left(\mu + \frac{\mu_t}{\sigma_k} \right) \frac{\partial k}{\partial x_j} \right] + \rho(P_k - \varepsilon)$$

$$\frac{\partial(\rho \varepsilon)}{\partial t} + \frac{\partial(\rho \varepsilon u_j)}{\partial x_j} = \frac{\partial}{\partial x_j} \left[\left(\mu + \frac{\mu_t}{\sigma_\varepsilon} \right) \frac{\partial \varepsilon}{\partial x_j} \right] + \frac{\rho}{k} (C_1 P_k - C_2 \varepsilon) \tag{7}$$

where P_k is the generation of turbulence kinetic energy defined as

$$P_k = \frac{\mu_t}{\rho} \left(\frac{\partial u_i}{\partial x_j} + \frac{\partial u_j}{\partial x_i} \right) \frac{\partial u_i}{\partial x_j} \tag{8}$$

The model constants $C_\mu, C_1, C_2, \sigma_k, \sigma_\varepsilon$ have the values: $C_\mu=0.09, C_1=1.44, C_2=1.92, \sigma_k=1.0, \sigma_\varepsilon=1.3$.

2.2. CFD Numerical Method

Based on the finite volume method, the flow equations are spatially discretized with the convection term of second order upstream scheme, and other terms are discretized with the central difference scheme. To obtain a converged solution, the SIMPLEC algorithms is used to separately solve the momentum equations and the continuity equation, additionally, at the end of each solver iteration, the residual for each of the conserved variables is computed and the convergence is judged if the maximal residual decreases to 10⁻⁵.

2.3. CFD Mesh Model

The structure schematic drawing of tee is shown as Fig. (1a). The inner diameters D_1 of the main inlet pipe and outflow pipe are the same as 101.6 mm, and the inner diameter D_2 of branch pipe is 50.8 mm. As the hypothesis of full developed flow in the tee, the length of each straight pipe should be more than 3 times of the diameter, and $L=1800\text{mm}, L_1=720\text{mm}, L_2=500\text{mm}, L_3=360\text{mm}$. The fluid is liquid with the density of 1000 kg/m³, and the viscosity is 0.001Pa·s. To establish the CFD mesh model, the flow zone is divided into several subdomain for meshing. The region around tee junctions is meshed with tetrahedrons element for its good adaptability to the unstructured model, and hexahedron elements are generated in other zones to reduce the number of elements. As the energy loss is mostly caused in junctions and the simulation should be independent of mesh, the tetrahedrons element is much finer and the number of element is determined with checking computations. The mesh model shown in Fig. (1b) includes 25763 tetrahedrons elements and 56592 hexahedron elements.

The flow boundary conditions include velocity inlet at inlet 1 and inlet 2, where the velocity vectors are defined

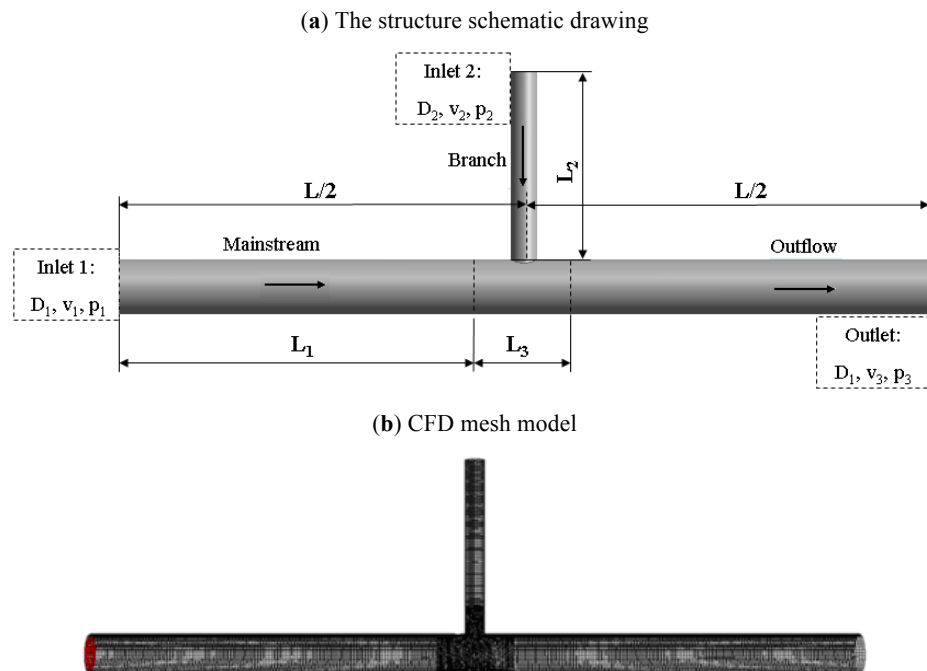


Fig. (1). Tee model.

with v_1 , v_2 , and one pressure outlet at outlet with a specified static pressure p_0 . The wall is static and a no-slip condition is specified.

Considering that the total head loss from the inlet 1 to outlet includes frictional head loss and local head loss of tee, the straight pipe model is built as Fig. (2) to compare energy loss with the tee model.



Fig. (2). CFD model of straight pipe.

3. SIMULATION RESULT AND ANALYSIS

When the inlet velocity v_1 is equal to 2m/s, partial streamlines are shown in Fig. (3). It shows that the branch with the inlet velocity of 0.1 m/s is on the upper part of flow channel due to the jacking role of the mainstream, and it flows to the pipe center gradually during the mixing of two streams. However, the branch with the inlet velocity of 1m/s forces the mainstream to significantly turn to the opposite side of junction after it flows into the junction, and a vortex is formed at the downstream of junction as a result Fig. (4).

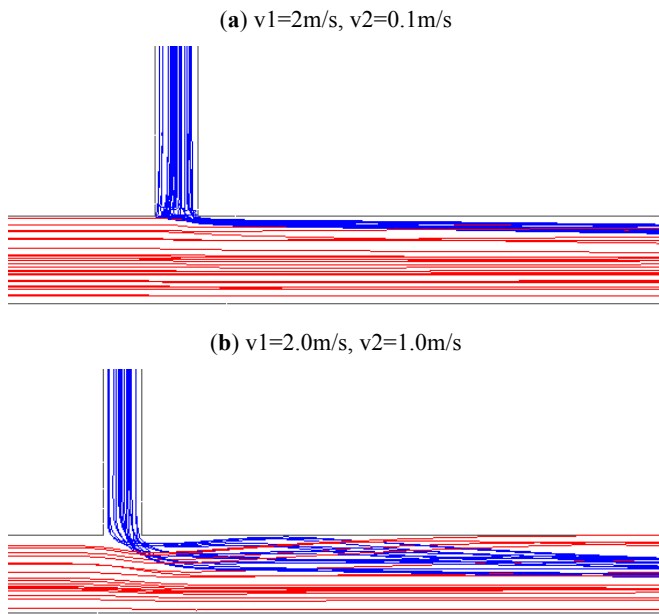


Fig. (3). Partial streamlines on the symmetry plane.

Fig. (5) shows the static pressure filed on the symmetry. When the velocity of branch is higher, junction of tee has a larger effect on the surrounding pressure, which is characterized by the increasing of pressure in the upstream and decreasing of pressure in the downstream of junction. Additionally, a negative pressure zone usually exists at the same side of junction.

Fig. (6) shows the cross-sectional area-weighted average pressures along the main stream. There is a maximal average pressure value in 0.9m where the center axis of the branch locates in, and the average pressure increase slightly at the range of about 1 time the pipe diameter in the upstream. However, the pressure in the downstream decreases significantly, and it is affected by the junction more greatly as the branch velocity increases. With the branch velocity of

1.0 m/s, downstream becomes stable when the distance from the axis of branch is larger than 3 times the pipe diameter.

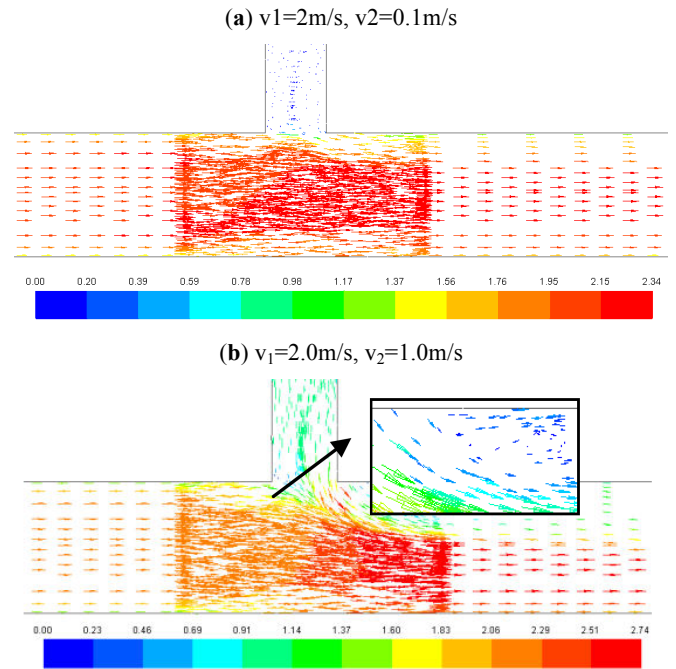


Fig. (4). Velocity field on the symmetry plane (m/s).

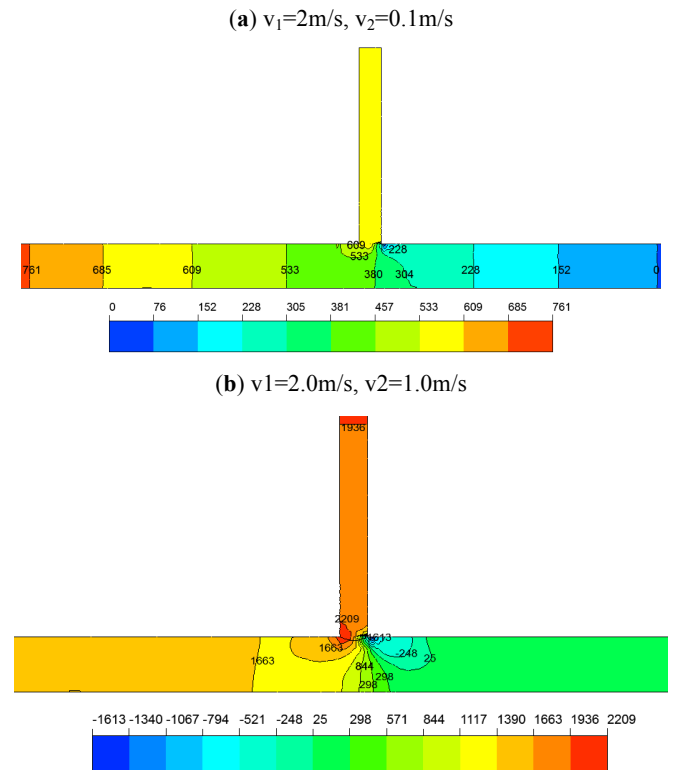


Fig. (5). Pressure field on the symmetry plane (Pa).

4. HEAD LOSS OF TEE

When the average pressures at upstream and downstream of junction is determined, the local head loss h_j can be calculated with the pressure drop,

$$h_j = \frac{p_3 - p_1}{\rho g} - h_{f1} - h_{f2} \quad (9)$$

Then the local resistance coefficient ζ_j is calculated

$$\zeta_j = \frac{2gh_j}{v_3^2} \quad (10)$$

where p_3 and p_1 are fluid pressures on outlet and inlet 1. ρ denotes the fluid density, and g is gravitational acceleration. h_{f1} and h_{f3} are upstream frictional head loss and downstream frictional head loss, respectively, they can be written as

$$h_{f1} = \lambda_1 \frac{L/2}{D_1} \frac{v_1^2}{2g} \quad h_{f3} = \lambda_3 \frac{L/2}{D_1} \frac{v_3^2}{2g} \quad (11)$$

where v_3 is the outlet velocity, λ_1 and λ_3 are frictional resistance coefficients based on velocity v_1 and v_3 , respectively, which are determined by the simulation of the straight pipe flow.

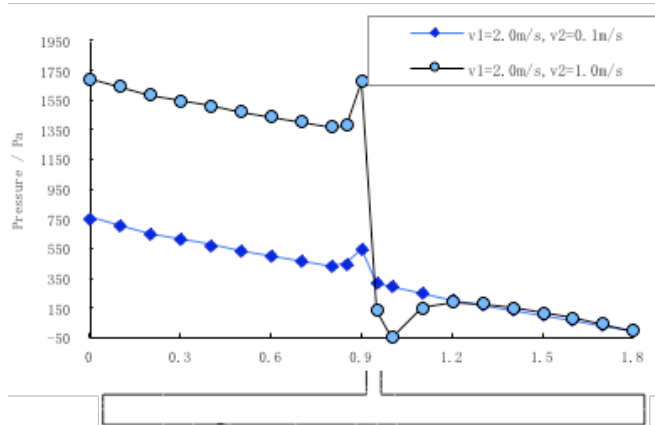


Fig. (6). Cross-sectional area-weighted average pressures along the main steam.

The frictional head loss h_f is calculated with the pressure drop Δp of straight pipe shown in Fig. (2),

$$h_f = \lambda \frac{L}{D} \frac{v^2}{2g} = \frac{\Delta p}{\rho g} \quad (12)$$

where λ is frictional resistance coefficient, L and d are length and diameter of straight pipe respectively. Δp is the pressure drop between the inlet and outlet, and λ is attained as followed

$$\lambda = \frac{2\Delta p D}{\rho v^2 L} \quad (13)$$

Fig. (7) shows the frictional resistance coefficients calculated at different velocities. When the inlet velocity increases from 1 m/s to 12 m/s, the frictional resistance coefficient λ declines from 0.0207 to 0.0133, following the power function relationship, which can be written as

$$\lambda = 0.0205v_3^{-0.178} \quad R^2 = 0.9989 \quad (14)$$

Through Eq. (14), the frictional resistance coefficient for different segment is determined at different flow conditions, and the simulation result is shown in Table 1.

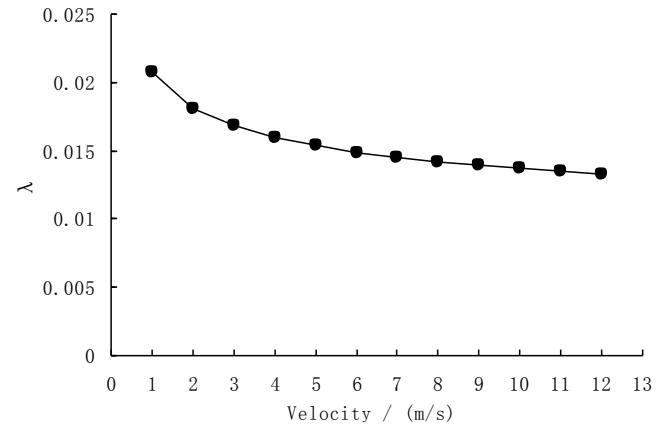


Fig. (7). Frictional resistance coefficient changes with inlet velocity.

It is noted that Re number is calculated according to v_3 and D_1 , and the pressure p_3 of outlet is 0.

The pressure drop p_1-p_3 is also tested for the tee shown in Fig. (8), of which the size is the same as the CFD model, and the data is listed in Table 2. It shows that the simulation is in good agreement with the test as the maximum relative deviation is less than 0.087. This proves that the CFD numerical method adopted is effective.

The curve of local resistance coefficient changed with Re number is shown as Fig. (9). At flow conditions of No. 1-11, the coefficient raises with the increase of inlet velocity of branch when the velocity of the mainstream is fixed. However, the coefficient decreases when the inlet velocity of mainstream increases and the other is fixed at conditions of No. 11-13. This indicates that the flux ratio of branch to mainstream has a great influence on the local resistance coefficient.

Fig. (10) shows the relationship curve of local resistance coefficient and flux ratio of branch to mainstream. The coefficient increases monotonically with increasing ratio, and they nearly follows the quadratic polynomial, which can be written as

$$\zeta_j = -4.2527\beta^2 + 3.521\beta + 0.0087 \quad R^2 = 0.9999 \quad (15)$$

CONCLUSION

In summary, we have simulated the flow field inner tee for revealing the cause of local head loss. The flow characteristic of tee junction is that the branch forces the mainstream to turn to the opposite side of the junction, and the pressure drop between upstream and downstream increases. As the pressure drop includes the frictional head loss and local head loss, the frictional resistance coefficient is determined through the simulation of straight pipe, and the coefficient decreases from 0.0207 to 0.0133 when the inlet velocity increases from 1 m/s to 12 m/s, which follows the power function relationship.

By eliminating the frictional head loss, the local resistance coefficient of tee is attained at different flow conditions, and a relationship of quadratic polynomial between the coefficient and the flux ratio of branch to mainstream is obtained, which objectively reflected the influence of branch on mainstream.

Table 1. CFD simulation results.

No.	Inlet 1			Inlet 2	Outlet		Local Resistance Coefficient ζ_j	Re (Based on v3)	Flux Ratio of Inlet 2/Inlet 1
	p1/ Pa	v1 /m·s-1	λ_1	v2/ m·s-1	v3/ m·s-1	λ_3			
1	658	2.0	0.01812	0	2.00	0.01812	0.00783	203200	0
2	753	2.0	0.01812	0.10	2.02	0.01808	0.05050	205730	0.013
3	856	2.0	0.01812	0.20	2.05	0.01804	0.09462	208273	0.025
4	958	2.0	0.01812	0.30	2.07	0.01800	0.13629	210816	0.038
5	1059	2.0	0.01812	0.40	2.10	0.01796	0.17569	213358	0.050
6	1162	2.0	0.01812	0.50	2.13	0.01793	0.21349	215900	0.063
7	1265	2.0	0.01812	0.60	2.15	0.01789	0.24986	218442	0.075
8	1368	2.0	0.01812	0.70	2.18	0.01785	0.28443	220984	0.088
9	1473	2.0	0.01812	0.80	2.20	0.01782	0.31828	223525	0.100
10	1581	2.0	0.01812	0.90	2.23	0.01778	0.35138	226066	0.113
11	1690	2.0	0.01812	1.00	2.25	0.01774	0.38378	228600	0.125
12	2256	2.5	0.01741	1.00	2.75	0.01712	0.31733	279407	0.100
13	2887	3.0	0.01681	1.00	3.25	0.01662	0.27245	330207	0.083
14	4480	3.5	0.01640	1.50	3.88	0.01611	0.33549	393713	0.107
15	6264	4.5	0.01568	1.50	4.88	0.01546	0.27175	495313	0.083
16	8518	5.0	0.01536	2.00	5.50	0.01513	0.31662	558820	0.100
17	11106	5.5	0.01513	2.50	6.13	0.01485	0.35239	622325	0.114
18	14018	6.0	0.01490	3.00	6.75	0.01459	0.38173	685830	0.125
19	15489	6.5	0.01469	3.00	7.25	0.01441	0.35708	736631	0.115
20	18888	7.0	0.01451	3.50	7.88	0.01420	0.38176	800136	0.125
21	22621	7.5	0.01432	4.00	8.50	0.01401	0.40331	863641	0.133
22	26662	8.0	0.01419	4.50	9.13	0.01383	0.42123	927147	0.141
23	28675	8.5	0.01401	4.50	9.63	0.01370	0.40090	977947	0.132
24	30735	9.0	0.01391	4.50	10.13	0.01358	0.38191	1028748	0.125
25	35430	9.5	0.01373	5.00	10.75	0.01343	0.39915	1092254	0.132
26	37688	10.0	0.01368	5.00	11.25	0.01332	0.38177	1143058	0.125

The present work also compares the simulation and test, and there is a good agreement between them with the maximum relative deviation of 0.087, which proves that the simulation is effective.



Fig. (8). Hydraulic test of tee.

Table 2. Comparison of pressure drop between test and simulation.

No.	v1 (m/s)	v2 (m/s)	p1-p3		Relative Deviation
			Test	Simulation	
1	2	0.3	910	958	0.053
2	2.5	1	2100	2256	0.074
3	3.5	1.5	4300	4480	0.042
4	4.5	1.5	5900	6264	0.062
5	7	3.5	17380	18888	0.087
6	8	4.5	24700	26662	0.079

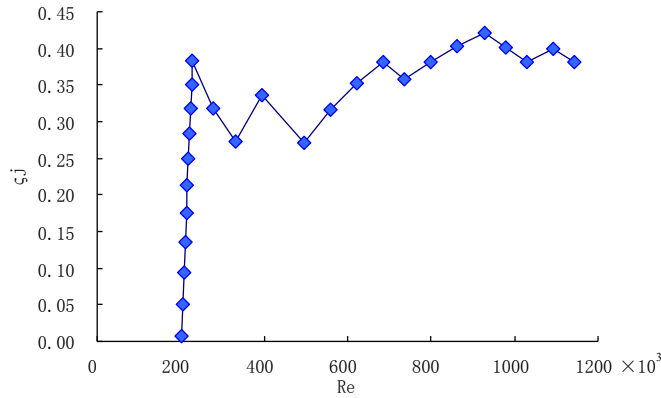


Fig. (9). Local and frictional resistance coefficient of tee.

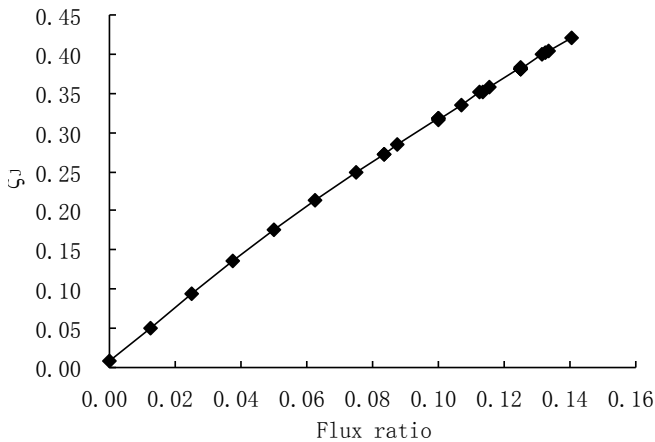


Fig. (10). Local and frictional resistance coefficient of tee.

CONFLICT OF INTEREST

The authors confirm that this article content has no conflict of interest.

ACKNOWLEDGEMENTS

This work is supported by the Ministry of Education Doctoral Fund, China (No.20114220110001) and the National Natural Science Foundation of China (No. 61170031).

REFERENCES

- [1] S. Wu, Z. Zhouzhijie, and L. Duwenbin, "Experimental study of the tee local resistance characteristics", *Journal of China Engineering Thermal Physics Flows (Multiphase Flow)*, 2010.
- [2] B. Jorgen, and M. Tor-Goran, "Pressure drops in T-junctions a comparison," *ASHRAE Transaction*, vol.106, no.1, pp. 359-364, 2000.
- [3] X. Yang, "Three Bifurcation Pipe Flow Numerical Simulation and Flow Characteristics", China, D. Tianjin University, 2004.
- [4] P. Liu, Q. Qu, Z. Wang, Z. Hongmei. "Numerical simulation on hydro-dynamic characteristics of bifurcation pipe th internal-crescentirb", *Journal of Hydraulic Engineering*, vol. 35, no. 2, pp. 42-46, 2004.
- [5] J. Chen, H. Lü, X. Shi, Z. Delan, W. Wene, "Numerical simulation and experimental study on hydrodynamic characteristics of T-type pipes", *Transactions of the Chinese Society of Agricultural Engineering (Transactions of the CSAE)*, vol. 28, no. 5, pp. 73-77, 2012.
- [6] L. Li, Y. Li, J. Huang, H. Zhongzhi. "Numerical simulation and experim entalstudy on waterflow in Y-type tube" *Journal of Hydraulic Engineering*, vol.32, no.2, pp. 49-53, 2001.
- [7] G. Mao, J. Zhang, W. Cheng, H. Yunjin, P. Liuping, C. Lifen, "Experimental study and 3-D numerical simulation on water flow in Y-type pipe", *Hydroelectric Power Journal*, vol. 24, no. 2, pp. 17-20, 2005.
- [8] B. E. Launder, and D. B. "Spalding, *Lectures in mathematical models of turbulence M*, Academic Press, London, 1972.

Received: February 17, 2014

Revised: March 21, 2015

Accepted: June 9, 2015

© Zhang et al.; Licensee Bentham Open.

This is an open access article licensed under the terms of the (<https://creativecommons.org/licenses/by/4.0/legalcode>), which permits unrestricted, non-commercial use, distribution and reproduction in any medium, provided the work is properly cited.